Article

Neuron

Bidirectional Control of Generalized Epilepsy Networks via Rapid Real-Time Switching of Firing Mode

Highlights

- TC output is synchronized, phasic, and rhythmic during spontaneous SWDs
- Unilaterally toggling TC phasic spiking via eNpHR induces bilateral SWDs
- Unilaterally toggling TC tonic spiking via SSFO bilaterally aborts SWDs
- Unilaterally suppressing TC output via eNpHR bilaterally shortens SWDs

Authors

Jordan M. Sorokin, Thomas J. Davidson, Eric Frechette, Armen M. Abramian, Karl Deisseroth, John R. Huguenard, Jeanne T. Paz

Correspondence

jeanne.paz@gladstone.ucsf.edu

In Brief

Here Sorokin et al. investigate the roles of phasic and tonic firing modes of thalamocortical relay cells in absence epilepsy and discover that unilaterally toggling TC phasic firing initiates bilateral absence seizures, while switching to tonic aborts seizures in real time.

Sorokin et al., 2017, Neuron *93*, 194–210
January 4, 2017
http://dx.doi.org/10.1016/j.neuron.2016.11.026

CellPress

CellPress

Neuron
Article

Bidirectional Control of Generalized Epilepsy Networks via Rapid Real-Time Switching of Firing Mode

Jordan M. Sorokin,[1,2] Thomas J. Davidson,[3] Eric Frechette,[2] Armen M. Abramian,[2] Karl Deisseroth,[4] John R. Huguenard,[2] and Jeanne T. Paz[5,6,7,*]

[1]Stanford Neurosciences Graduate Training Program, Stanford University, Stanford, CA 94305, USA
[2]Department of Neurology and Neurological Sciences, Stanford University School of Medicine, Stanford, CA 94305, USA
[3]Howard Hughes Medical Institute and Center for Integrative Neuroscience, University of California San Francisco, San Francisco, CA 94158, USA
[4]Department of Bioengineering, Stanford University School of Medicine, Stanford, CA 94305, USA
[5]Gladstone Institutes, San Francisco, CA 94158, USA
[6]Department of Neurology, University of California San Francisco, San Francisco, CA 94158, USA
[7]Lead Contact
*Correspondence: jeanne.paz@gladstone.ucsf.edu
http://dx.doi.org/10.1016/j.neuron.2016.11.026

SUMMARY

Thalamic relay neurons have well-characterized dual firing modes: bursting and tonic spiking. Studies in brain slices have led to a model in which rhythmic synchronized spiking (phasic firing) in a population of relay neurons leads to hyper-synchronous oscillatory cortico-thalamo-cortical rhythms that result in absence seizures. This model suggests that blocking thalamocortical phasic firing would treat absence seizures. However, recent in vivo studies in anesthetized animals have questioned this simple model. Here we resolve this issue by developing a real-time, mode-switching approach to drive thalamocortical neurons into or out of a phasic firing mode in two freely behaving genetic rodent models of absence epilepsy. Toggling between phasic and tonic firing in thalamocortical neurons launched and aborted absence seizures, respectively. Thus, a synchronous thalamocortical phasic firing state is required for absence seizures, and switching to tonic firing rapidly halts absences. This approach should be useful for modulating other networks that have mode-dependent behaviors.

INTRODUCTION

Reciprocal communication between thalamus and cortex is critical to normal sensory experience (Steriade, 2000; Steriade et al., 1993; Contreras and Steriade, 1995), and disorders in these circuits are associated with seizures (Huguenard, 1999; Beenhakker and Huguenard, 2009; Kostopoulos, 2000) and altered cognitive processing (Buzsáki and Watson, 2012). The firing modes of individual thalamocortical (TC) and corticothalamic (CT) neurons, which can fluctuate between burst and tonic firing, can alter cortico-thalamo-cortical (CTC) function (Castro-Alamancos, 2004; Steriade et al., 1993; Steriade, 2000). One form of epilepsy associated with changes in firing mode is generalized absence epilepsy. Genetic animal models of this disorder display stereotyped bilaterally synchronous spike-wave discharge (SWD) electrographic seizure activity and episodes of behavioral arrest (Danober et al., 1998; Coenen et al., 1992; Marescaux et al., 1992). SWDs, in both human patients and animal models, result from abnormally synchronous oscillations in CTC networks (for review, see Danober et al., 1998; Beenhakker and Huguenard, 2009). Within the CTC circuit, the necessity of TC versus CT output and firing mode in generating and/or maintaining global epileptic activity has been debated (Meeren et al., 2005; Polack and Charpier, 2006; Huguenard, 1999). One current working model is that CT output is sufficient to initiate and maintain SWDs and that active TC phasic output (see Experimental Procedures) is *not* necessary (Polack et al., 2007; Polack and Charpier, 2006; Pinault, 2003). This conclusion, obtained by multiple research groups, is based in part on the findings that (1) intracortical infusions of tetrodotoxin (TTX), lidocaine, or ethosuximide can effectively suppress SWDs in epileptic rats (Polack et al., 2009; Manning et al., 2004; Sitnikova and van Luijtelaar, 2004), while intra-thalamic delivery of these compounds is less effective (Richards et al., 2003; Polack et al., 2009) and (2) TC neurons in epileptic rats and cats are silent or only fire sparse single spikes during SWDs due to the shunting output of GABAergic reticular thalamic (RT) neurons (Timofeev et al., 1998; Timofeev and Steriade, 2004; Steriade and Contreras, 1995; Pinault et al., 1998; Pinault, 2003; Polack and Charpier, 2006).

An alternate view is that phasic TC firing promoted by T-current-dependent post-inhibitory rebound (PIR) bursts (Jahnsen and Llinás, 1984; Coulter et al., 1989) is required for SWDs. This view is supported by the observation that lesions of the RT, which normally drives TC PIR bursts (for review, see Huguenard and McCormick, 2007), reduce both SWDs and high-voltage neocortical spindles (Avanzini et al., 1993; Buzsáki et al., 1988). Further, many in vitro studies using rodent thalamic slices (Huguenard and Prince, 1994; Huguenard and McCormick, 1992; Sohal et al., 2000) strongly argue that the intra-thalamic RT-TC loop

undergoes prominent seizure-related oscillatory activity with burst firing in both RT and TC cells. In contrast with these in vitro studies, researchers have surprisingly found in vivo that RT output tends to shunt TC activity rather than promote oscillatory PIR bursts (Steriade and Contreras, 1995). However, these in vivo findings were obtained in animals under anesthesia, which can alter CTC firing dynamics.

While the specific contribution of TC phasic firing has not been shown, previous studies have shown that the thalamus at large plays a role in SWDs. For instance, pharmacological manipulations, such as intra-thalamic infusion of GABA agonists into Genetic Absence Epilepsy Rats from Strasbourg (GAERS), promoted SWD occurrence, while KCl, GABA, and glutamate antagonists prevented SWDs (Paz et al., 2007; Cope et al., 2009; Danober et al., 1998; Marescaux et al., 1992). Further, lesions to certain thalamic nuclei affect SWDs of the same hemisphere (Avanzini et al., 1993; Vergnes and Marescaux, 1992), and lesions and pharmacological manipulations of the basal ganglia and neuromodulator pathways affect SWDs (Danober et al., 1993, 1998). Nonetheless, these results stem from non-specific manipulations that confirm only (1) the necessity of a fully intact CTC network for SWD expression and (2) that modulatory pathways, which affect diffuse brain regions and cognitive states, influence absence seizures. Thus, these studies do not address the specific roles of various pathways and firing states in the CTC network for SWDs. These controversies lead to three questions to be addressed in this study, as follows.

Why is it important to determine whether the thalamus is actively involved in SWDs? If the thalamus simply follows cortically generated SWDs, then there is little point in further studying thalamic channelopathies or developing novel antiepileptic therapies that target TC firing. On the other hand, if phasic firing in TC cells does contribute to SWD generation, then therapies that target phasic firing may have powerful anti-absence effects. Given that phasic TC output is mediated by Cav3.1 T-channels, and that novel, selective T-type channel blockers (compared to the non-selective blocker ethosuximide) (Gomora et al., 2001) are under development (Dreyfus et al., 2010), then those that specifically target Cav3.1 may be legitimate treatments for absence epilepsy and potentially other disorders involving aberrant TC phasic firing, perhaps with fewer side effects.

What are potential explanations for opposing findings? Previous studies that were performed under anesthesia, neuroleptanalgesia, or in brain slices, which allow for stable high-quality intracellular recordings, have yielded important insights on intrinsic membrane properties and subthreshold synaptic activities from epileptic cortical and thalamic (TC and RT) neurons that cannot be obtained with extracellular recordings. However, such preparations affect CTC network dynamics. Moreover, given the adjacency and reciprocity of TC and CT projection pathways (Jones, 2002; Adams et al., 1997), it is challenging to specifically isolate the contributions of the thalamus and the cortex via techniques used in other previous studies (lesions, pharmacology, and electrical stimulations), as these can indirectly affect neighboring networks.

How can the opposition be resolved? Recent advances in optogenetic tools now enable cell-type-specific manipulations of firing mode in real time, positioning us to resolve these long-standing issues regarding the necessity of active TC phasic output for the maintenance of naturally occurring absence seizures during free behavior.

Here we demonstrate that TC neurons rhythmically fire synchronized, phasic clusters of action potentials that are time-locked with natural SWDs in freely behaving mice and rats and that such TC phasic output is necessary to maintain SWDs and behavioral absences. We first used electrophysiology to reveal the endogenous properties of TC neurons in behaving rodents. Then, we applied novel optogenetic approaches to selectively manipulate the *unilateral* TC component of the CTC circuit to determine whether TC phasic firing alone is sufficient to initiate and necessary to maintain generalized SWDs. We manipulated the firing modes of TC neurons in the ventrobasal (VB) complex—the primary somatosensory relay center (Chmielowska et al., 1989)—in healthy mice and rats and in two genetic models of absence epilepsy: Stargazer (STG) mice (Lacey et al., 2012; Noebels et al., 1990) and Wistar Albino Glaxo rats from Rijswijk (WAGRij) (Coenen et al., 1992; Sarkisova and van Luijtelaar, 2011).

RESULTS

Unilaterally Manipulating TC Output Is Sufficient to Alter Bilateral Cortical States in Non-epileptic Rats

Normal oscillatory output from the thalamus, which is believed to recruit ipsilateral cortical activity (Steriade et al., 1993), is primarily driven by RT-mediated PIR bursts in TC neurons (Steriade et al., 1993; Cox et al., 1997). To test whether *unilateral* TC oscillatory output can drive *bilateral* cortical rhythms, we expressed an inhibitory opsin, halorhodopsin (eNpHR3.0) (Gradinaru et al., 2008) unilaterally in excitatory VB TC neurons in non-epileptic rats. In vitro photoinhibition of eNpHR-expressing TC neurons in acute brain slices with brief 594 nm pulses at various frequencies (see Experimental Procedures) reliably drove robust PIR bursts (Jahnsen and Llinás, 1984) with ~25 ms latencies (Figures 1A and 1C) mediated by T-type calcium channels (Coulter et al., 1989). Our in vitro experiments documented unambiguous single-cell, multi-spike PIR bursts after each and every 594 nm pulse within the pulse trains (Figure 1A).

Our in vivo results were consistent with this finding, where we recorded multi-unit (MU) activity with chronic optrode devices (Yizhar et al., 2011) implanted in the right VB of adult non-epileptic rats and mice along with electrocorticogram (ECoG) electrodes in ipsilateral and contralateral cortical hemispheres, as described in Paz et al. (2013) (see Experimental Procedures). We found that unilaterally delivered 594 nm pulse trains at various frequencies (see Figure 1F) robustly drove phasic action potentials in a local population of TC cells (that we will refer to as "clustered spiking" for simplicity; see Experimental Procedures). Strikingly, these pulses drove 12 Hz ECoG oscillations in *both* hemispheres (Figures 1B–1E), suggesting that unilateral TC clustered spiking can evoke bilateral thalamocortical network responses independent of the stimulation frequency (Figure 1F). Although we did not isolate individual single units from our recordings, our results clearly show that 594 nm pulses organize MU TC activity into high-frequency clusters with similar post-light latencies to in vitro T-current-mediated PIR bursts (~25 ms; see Figures 1A and 1B; Figure S1A). In some cases, just a few light pulses

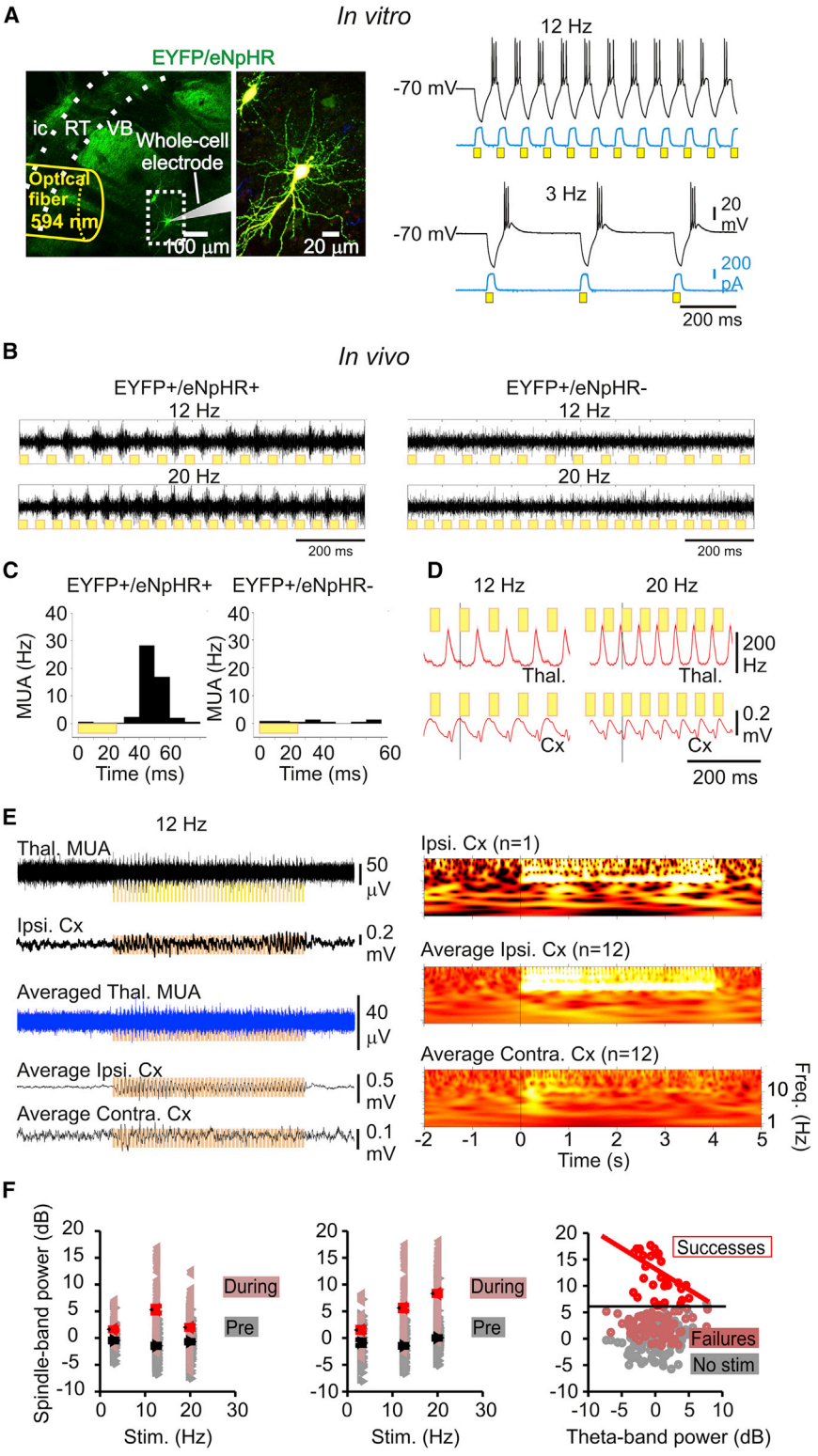

Figure 1. 12 Hz Train of 594 nm Light Drives Sleep-like Spindles in Normal Rats

(A) In vitro 594 nm trains induced eNpHR currents (blue) and rhythmic hyperpolarizations (black) followed by PIR bursts in TC neurons (right) expressing eNpHR-EYFP (left, image of recorded slice showing eYFP fluorescence in VB).

(B) In vivo 12 Hz 594 nm trains delivered via optrodes induced synchronized oscillatory TC firing in animals expressing EYFP-eNpHR (left), but not in controls (right).

(C) Quantification of multi-unit activity (MUA) following the light pulse in eNpHR+ and eNpHR− TC neurons in vivo.

(D) Superimposed averaged thalamic MUA rate and averaged cortical ECoG during 594 nm pulses.

(E) Representative single and average traces (left) and spectrograms (right) showing in vivo 594-nm-induced TC clusters drive 12 Hz cortical oscillations.

(F) 594 nm trains fail to produce cortical oscillations during theta rhythm. Left: ipsilateral cortical spindle power (dark red triangles) induced by thalamic optical stimulation. Bright red triangles: mean ± SE. Gray: prestim cortical spindle power. Black triangles: mean ± SE. Middle: contralateral cortical spindle power (dark red triangles) induced by thalamic optical stimulation. Right: 12 Hz light train is more likely to evoke strong cortical spindles (bright red circles) in the absence of cortical theta activity. After eliminating stimuli not inducing spindle power >2 SD above the mean power (dark red circles), the evoked spindle power and cortical theta power are negatively correlated (bright red line). Gray: power in the spindle band immediately prior to the stimulus. SD, ~3 dB. Pearson's R2 = 0.22 for the linear fit. p = 0.008, 10 trials, 3 animals.

(<10) initiated ECoG oscillations that outlasted the optical train, indicating that the oscillation, once initiated in thalamus, became fully established in the CTC circuit. The effect of evoking phasic TC output on cortical oscillations depended on the behavioral state of the animal: in awake animals during pronounced cortical theta rhythm (5–12 Hz), which is associated with attention, exploration, and learning (Buzsáki and Moser, 2013; Hasselmo et al., 2002), photoinhibition of TC cells still produced oscillatory TC clustered spiking, yet failed to induce cortical oscillations (Figure 1F).

These results establish that coordinated rhythmic firing of a group of TC cells, even unilaterally, can entrain a global network CTC oscillator.

TC Firing Mode Switches from Tonic to Phasic during Spontaneous SWDs

To quantify innate TC firing behavior during spontaneous SWDs, we recorded ECoG (Figure 2A, top) and MU activity from the VB (Figure 2A, bottom) in epileptic WAGRij rats. All in vivo recordings were obtained from animals in states of quiet wakefulness. These rats

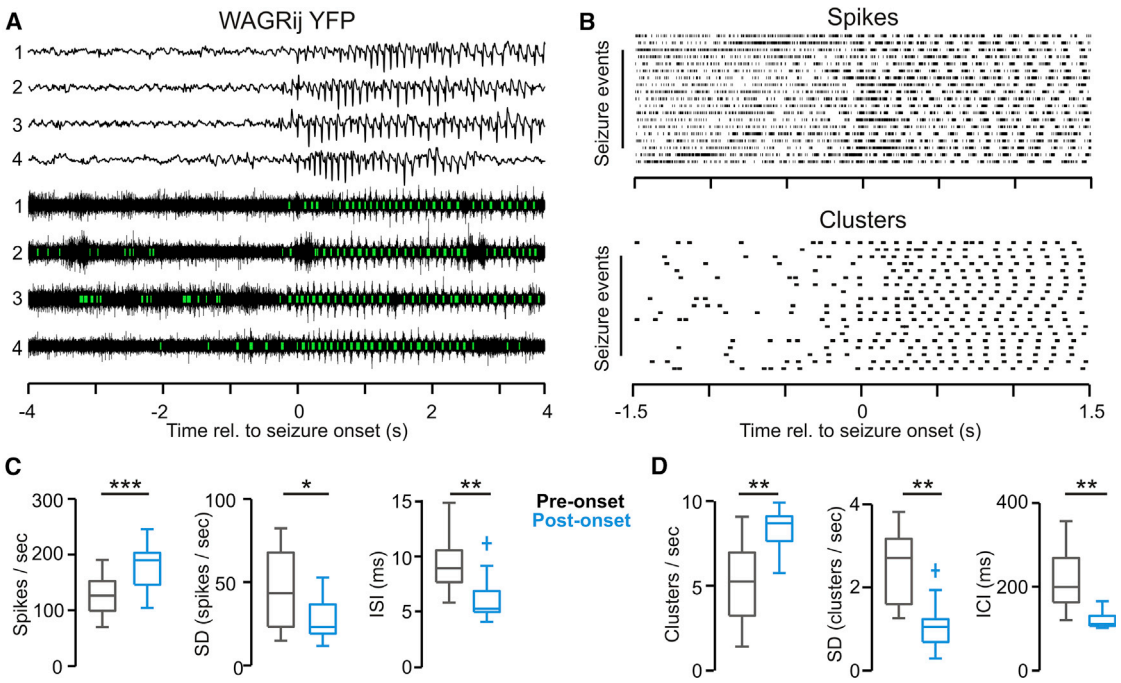

Figure 2. VB Displays Rhythmic, High Firing Rate Output throughout the Duration of Naturally Occurring Seizures

(A) Example ipsilateral ECoG (top) and thalamic multi-unit activity (bottom) with detected clusters (green) from four consecutive spontaneous seizures in a WAGRij-YFP rat.

(B) Rasters of detected spikes (top) and spike clusters (bottom) from the same animal/trial as in (A).

(C) The population spike rate (left), intra-trial SD of the spike rate (middle), and the inter-spike interval (right) averaged over 2 s windows prior to the seizure onset (gray) and following the seizure onset (blue) across all WAGRij-YFP animals. Note that the population spike rate actually increases during seizures, though becomes highly organized and phasic.

(D) The cluster rate (left), intra-trial SD of the cluster rate (middle), and the inter-cluster interval (right) across all WAGRij-YFP animals. n = 13 trials, 3 animals; Wilcoxon signed-rank test; *$p \leq 0.05$, **$p \leq 0.01$, ***$p \leq 0.001$.

See also Figure S5 and Table S1.

displayed highly stereotyped seizures, with prominent SWDs in the ECoG and robust, rhythmic TC clustered spikes time-locked to the ECoG (Figures 2A and 2B), which were infrequent and disorganized during inter-ictal periods. Interestingly, the overall rate of TC firing and the occurrence of clusters increased from pre-ictal to ictal periods in all rats (Figures 2C and 2D, left), with low variance among SWDs (Figures 2C and 2D, middle). Additionally, the inter-spike interval (ISI) decreased (Figure 2C, right) due to the organization of MU spikes into clusters. Most notably, the inter-cluster interval (ICI) became very regular (~100–120 ms, Figure 2D, right), matching the principle oscillatory frequency of rodent SWDs (Danober et al., 1998; Coenen et al., 1992).

Unilaterally Driving TC Phasic Firing Induces Generalized Absence Seizures and Behavioral Arrest in Epileptic Rodents

Given that absence seizures appear to emerge from similar elements of the thalamocortical network that drive normal oscillations as in sleep spindles (Kostopoulos, 2000; Beenhakker and Huguenard, 2009), we next investigated whether selectively driving TC phasic firing in epileptic animals could initiate SWDs. We expressed eNpHR-eYFP unilaterally in TC neurons of STG mice and WAGRij rats and delivered 8 Hz pulses of 594 nm light to TC neurons to mimic the fundamental frequency of rodent absence seizures (van Luijtelaar and Coenen, 1986; Noebels et al., 1990). Repetitive 594 nm (but not sham) pulses produced phasic clustered spikes in TC neurons, with similar post-light latencies (~28 ms) to our in vitro results (Figure 3G; Figure S1A). Robust CTC oscillations were detected in the thalamic local field potential (LFP) and cortical ECoG in both mouse and rat models of epilepsy (Figure 3A; Figure S1B, bottom), which were not seen in eYFP-controls (Table S1). We discovered that unilateral photoinhibition initiated bilateral cortical SWDs with classic features of absence epilepsy: synchronous 8 Hz rhythmic activity and behavioral absences identical to spontaneously occurring seizures (Figure 3C; Movie S1) (van Luijtelaar and Coenen, 1986).

To compare the optically induced seizures to spontaneously occurring events, we used wavelet decomposition (Torrence and Compo, 1998) to analyze changes in ECoG power centered around five frequency bands (see Experimental Procedures). We found significant changes in broadband (BB), β, and Ø* power for both WAGRij and STG expressing eNpHR-eYFP, but not eYFP (Figures 3B and 3D; Table S1). The Ø* and β bands reflect the fundamental and harmonic frequencies, respectively, of SWDs

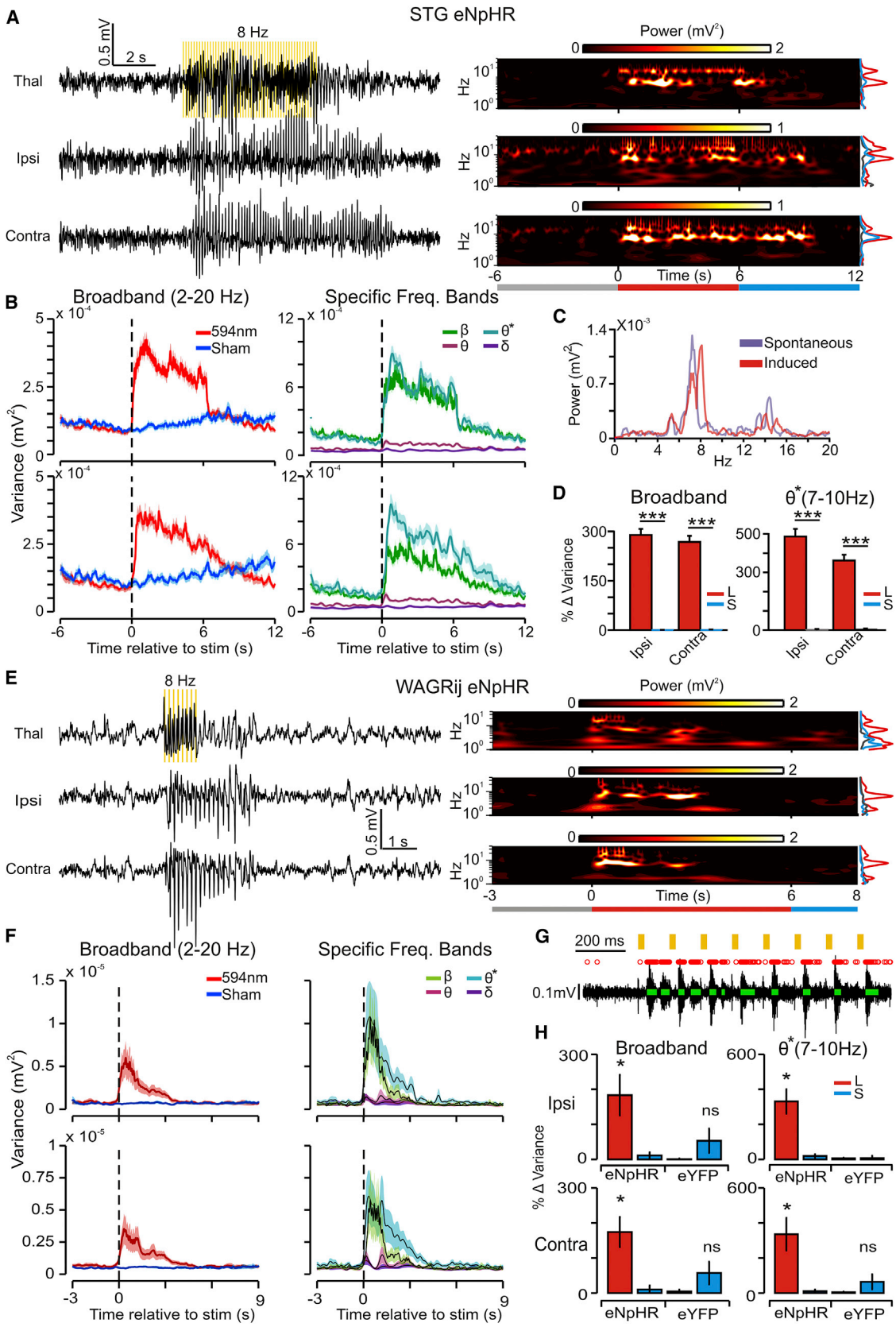

(legend on next page)

(see Figures 3A, 3C, and 3E). Notably, wavelet power in each ECoG channel increased relatively more for β and Ø* bands than it did for Ø, ∂, or BB (Figure 3B, right; Table S1), which was not evident in low-power 8 Hz controls or with 488 nm light (which does not strongly activate eNpHR) (Zhang et al., 2006) (Figures S2A–S2F; Movie S2).

Although long (~6 s) unilateral 8 Hz trains could drive bilateral SWDs, we wondered whether brief (1 s) 8 Hz trains could reproduce this result. Indeed, 1 s unilateral 8 Hz trains reliably drove bilateral SWDs with elevated Ø*, β, and BB power that outlasted the pulse train (Figures 3E and 3F; Table S1). Seizures were induced, on average, in 40%–50% of stimulations but only occurred by chance in ~0%–5% of cases following sham pulses and in eYFP animals (Figures S3B and S3C). Further, BB and Ø* ECoG power was elevated in both hemispheres after photoinhibition relative to sham and eYFP controls (Figure 3H). This is a striking result given that TC neurons of primary thalamic nuclei project exclusively to ipsilateral cortex (Jones, 2007).

Thalamic Induction of SWD Is Pulse-Frequency Invariant, and Even a Single Cluster of TC Spikes Can Initiate an SWD

We next asked whether various pulse frequencies could induce SWDs. We found that pulsed 594 nm light at 3, 12, and 20 Hz drove phasic clustered spikes in TC neurons that followed the pulse frequency (Figures 4A–4E) and increased the incidence of spike clusters compared to prestim periods and eYFP controls (Figures 4F and 4G). Although TC spike clusters followed the stimuli, we found that the different pulse frequencies consistently induced bilateral ECoG SWDs with maximal power in β and Ø* bands (Figure 4H; Table S1; Movie S3). These findings argue that the induced cortical oscillations do not simply reflect an extrinsic thalamic drive, but rather arise from intrinsic epileptic CTC network activity that is rapidly activated by a synchronous switch of TC neurons into a rhythmic, phasic state.

This raised the question: could a single, unilateral TC population action potential cluster also trigger a seizure? Surprisingly, one 50 ms pulse of 594 nm light delivered to WAGRij-eNpHR rats was sufficient to initiate sustained phasic TC firing at ~8 Hz (Figures 5C, 5D, and 5G), along with synchronous oscillations with elevated Ø* power in thalamic LFP and bilateral ECoG (Figures 5B, 5C, 5H, left, and 5I). These were accompanied by behavioral absences, which were not evoked in eYFP controls (Figures 5A and 5H, right) or with sham pulses (Figures 5E–5G). Induced SWDs showed a mean onset latency of 850 ms following the stimulus and duration of 3.24 s, as well as pronounced changes in Ø* and β power relative to Ø and ∂ (Figure 5H, bottom; Table S1). Seizures were induced in ~50% of stimulations on average versus ~0%–5% of cases with sham pulses and in eYFP controls (Figures S3A and S3D).

These results indicate that toggling phasic firing in TC neurons—even via a single unilateral cluster of action potentials—can initiate self-sustained bilateral epileptic activity that evolves irrespective of the frequency of direct, light-induced TC responses, likely by recruiting epileptic CTC networks (van Luijtelaar and Sitnikova, 2006).

Depolarizing TC Neurons Switches TC Firing Mode from Phasic to Tonic and Eliminates Clustered Spiking

Having shown that eNpHR photoinhibition reliably drives phasic firing of TC cells and CTC rhythms, we next asked: can the same TC pathway be targeted to destabilize ongoing rhythms? Indeed, closed-loop control of thalamus and hippocampus is sufficient to interrupt spontaneously occurring seizures in animal models of acquired epilepsy (Paz et al., 2013; Armstrong et al., 2013), and closed-loop cerebellar stimulation (Kros et al., 2015) and transcranial stimulation (Berényi et al., 2012) can disrupt SWDs. Despite these studies, the necessity of active TC phasic firing for SWD maintenance has never been studied in freely behaving rodents with absence epilepsy. To address this question, we developed our own closed-loop stimulation protocol (see Experimental Procedures) in order to unilaterally manipulate the TC firing mode during spontaneous seizures in both mice and rats.

We hypothesized that subthreshold depolarization of TC cells would enhance tonic firing associated with behavioral arousal (McCormick et al., 2015; McCormick, 1992; Steriade et al., 1993; Hirata and Castro-Alamancos, 2010; Poulet et al., 2012) and reduce the probability of phasic firing in response to SWD-related inhibitory RT output (Coulter et al., 1989; Huguenard, 2002; Huguenard and McCormick, 2007), and thus the ability to sustain an ongoing CTC oscillation. For this purpose, we expressed Stable Step Function Opsin (SSFO), a bistable

Figure 3. Rhythmic Activation of eNpHR in TC Drives Seizures in STG Mice and WAGRij Rats

(A) Left: example induced seizure from STG-eNpHR mouse with thalamic LFP (top), ipsilateral (middle), and contralateral (bottom) ECoG. Yellow bars indicate 8 Hz pulses of 594 nm light, delivered to the right VB. Right: time-frequency wavelet decomposition of traces. Right inset: average prestim, stim, and postsim power (times indicated by the colored bars below).

(B) Left: trial-averaged broadband (BB, 2–20 Hz) power (variance in this and all subsequent figures) over time for all laser (red) and sham (blue) trials. Right: trial-averaged power for laser-induced seizures, decomposed into different frequency bands (β = 10–20 Hz; Ø* = 7–10 Hz; Ø = 4–7 Hz; ∂ = 2–4 Hz).

(C) Contralateral ECoG from spontaneous (purple) and induced (red) seizures; note the peak power at ~7 Hz and harmonics at ~15 Hz in both conditions.

(D) Left: median BB power percent change ± SEM from prestim to stim periods for induced (red) and sham (blue) trials across STG mice. Right: median Ø* power percent change. (107/195 laser/sham events, 7 trials, 3 animals; $p < 0.001$, Wilcoxon rank-sum).

(E) Similar experiments reported in (A) but using a 1 s, 8 Hz pulse in WAGRij-eNpHR rats.

(F) The same analysis as in (B) applied to experiments in (E).

(G) Response of thalamic multi-unit (MU) activity in vivo to 594 nm pulses. Red X's, detected spikes; green bars, detected clusters (see Experimental Procedures). Note that clusters time-lock to 594 nm pulses.

(H) Median percent change in BB (left) and Ø* (right) power ± SEM for WAGRij-eNpHR and WAGRij-eYFP from prestim to stim for ipsilateral (top) and contralateral (bottom) ECoG. Red, laser; blue, sham ($p < 0.05$, Wilcoxon rank-sum; eNpHR: 7 trials, 4 animals; eYFP: 4 trials, 4 animals; see also Movie S1).

See also Figures S1–S3 and Table S1.

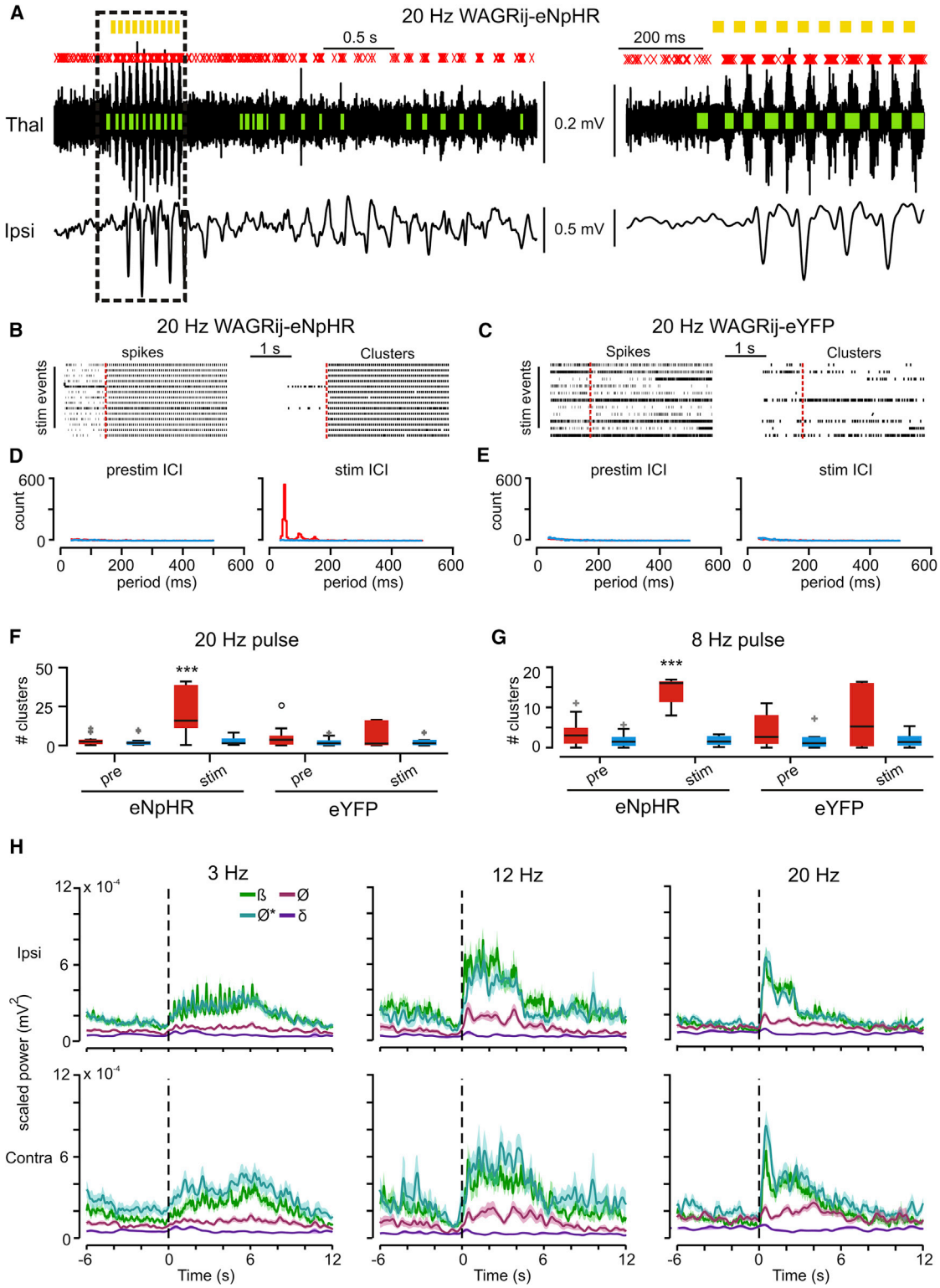

Figure 4. In Vivo Clusters from eNpHR Rodents Follow Various Pulse-Train Frequencies, yet Seizure-Specific ECoG Power Is Maximally Elevated

(A) TC multi-unit (MU) activity (top) and contralateral ECoG (bottom) from a WAGRij-eNpHR animal. MU spikes (red X's) cluster into phasic bouts (green bars) that consistently follow the 20 Hz pulses (yellow bars). Right: expanded trace from the highlighted region. Note that ECoG spike-wave discharges rapidly converge to ~8 Hz despite the 20 Hz pulse frequency.

(legend continued on next page)

depolarizing opsin (Yizhar et al., 2011), unilaterally in VB neurons in both STG mice and WAGRij rats.

We describe first the intracellular recordings from SSFO-expressing VB neurons in vitro from rats that had been used for successful in vivo recordings (see below and Experimental Procedures). SSFO activation and subsequent deactivation increased and decreased tonic firing in TC cells, respectively (Figures 6A and 6B). Notably, the SSFO activation strongly reduced the likelihood of eliciting TC PIR bursts, increased the likelihood of tonic spiking (Figures 6C and 6D), and reduced the burst index (BI), a measure of burst versus tonic firing propensity (Figures 6D and 6E).

Next, we determined the in vitro effects of SSFO on isolated thalamic network activity by recording extracellular MU activity in the VB of WAGRij rats from brain slices that preserved intrathalamic connectivity (Huguenard and Prince, 1994; Paz et al., 2011, 2013) (see Experimental Procedures). In control conditions (594 nm light only), internal capsule stimulation evoked intrathalamic oscillations with bouts of clustered spikes that lasted for many seconds (Figure 6F, left; Figures S4A and S4B). However, SSFO activation in TC cells by 488 nm light eliminated the evoked oscillations, increased desynchronized MU tonic firing (Figure 6F, right; Figure S4A and S4B), and reduced the oscillatory index (OI)—a measurement of the regularity and robustness of oscillations (Figures 6G and 6H), as well as the number of clusters per oscillation and the oscillation duration (Figures S4C and S4D). These data validate SSFO as a robust tool to toggle TC tonic firing and effectively desynchronize thalamic network oscillations.

Disrupting TC Phasic Firing In Vivo Desynchronizes Cortical Oscillations

We next asked whether toggling TC tonic firing in vivo could disrupt CTC rhythms. We developed an algorithm to unilaterally activate SSFO in the VB following SWD detection (see Experimental Procedures). Closed-loop SSFO activation reliably and rapidly eliminated TC clusters and toggled tonic firing, which was not observed with sham pulses (Figure 6J; Figures S4E–S4G and S5A–S5C) or in eYFP controls (Figure 6K; Figure S5D). The effect of unilaterally switching the firing mode from phasic to tonic on bilateral SWD was rapid and robust. SSFO activation bilaterally shortened SWDs in STG and WAGRij rats versus sham pulses, but not in eYFP controls (Figures 7E–7G; Figure S5A; Table S2; Movie S4), heightened arousal and exploratory behavior, and reduced Ø* (Figures 7A–7D) ECoG power; this did not occur with 594 nm light alone (Movie S5).

Thus, closed-loop toggling of TC tonic firing mode via SSFO-mediated depolarization is a novel and reliable mechanism to abolish synchronized TC phasic firing in vivo and desynchronize bilateral SWDs and behavioral absences. Moreover, our experiments show that phasic TC output is a consistent feature of spontaneous absence seizures (Figures 2 and 5I–5K; Figure S5A, left) and that such phasic firing is required for SWD maintenance.

Given the robustness of TC phasic firing during SWDs and the strong effects of SSFO activation, we wondered whether the TC output is necessary for SWD expression. To test this, we used a similar closed-loop protocol for our STG-eNpHR mice but delivered 594 nm light (see Experimental Procedures). eNpHR activation strongly reduced MU TC firing compared to sham (Figures S6A and S6B) and bilaterally shortened SWDs in all three STG-eNpHR mice (Figures S6C–S6F). In combination with our SSFO results, this experiment argues that the continued phasic TC output is necessary for SWD maintenance during free behavior.

DISCUSSION

We investigated the role of TC neurons in generating cortical rhythms relevant to non-epileptic and absence behavior. For this purpose, we developed two novel optogenetic strategies to drive or disrupt phasic and tonic firing states unilaterally in VB neurons with high temporal resolution. We demonstrate in non-anesthetized, freely behaving mice and rats that TC activity can bi-directionally control SWDs and behavioral absences in real time.

Specifically, we demonstrated that (1) TC firing is heightened and organized into phasic clusters during seizures, (2) unilaterally driving TC phasic firing can initiate bilateral CTC oscillations and SWDs, (3) switching TC firing mode from phasic to tonic is sufficient to globally terminate SWDs, and (4) reducing TC firing shortens SWDs. Finally, we demonstrated that TC clustered spiking is robust throughout spontaneous and evoked SWDs. These results were supported by in vivo and in vitro experiments and were validated in vitro in tissue from animals used for in vivo recordings.

The striking finding that a single TC spike cluster can initiate an SWD (Figure 5) suggests that the TC pathway can rapidly recruit global CTC oscillators. These results are in agreement with our previous studies using the GluA4 knockout mouse in which

(B) In vivo spike (left) and cluster (right) rasters from WAGRij-eNpHR before and during a 20 Hz train of 594 nm light (red bar = 594 nm onset).
(C) Same as (B), but for a WAGRij-eYFP control.
(D) Prestim (left) and during stim (right) inter-cluster interval (ICI) across all laser (red) and sham (blue) pulses for same animal as in (B), showing that bursts organize around ~50 ms.
(E) Same as (D), but for WAGRij-eYFP, demonstrating lack of cluster organization during the stim.
(F) Boxplots of the number of prestim (left) and stim (right) clusters during a 20 Hz pulse train across all recording trials for all animals, averaged on a per-trial basis for laser (red) and sham (blue) conditions. Only WAGRij-eNpHR show an elevated number of clusters during the laser stim period ($p < 0.001$, ANOVA, eNpHR: 10 trials, 4 animals; eYFP: 7 trials, 4 animals). °, not significant.
(G) Same as (F), but for 8 Hz ($p < 0.001$, ANOVA, eNpHR: 21 trials, 4 animals; eYFP: 11 trials, 5 animals).
(H) Average power across different frequency bands (β = 10–20 Hz; Ø* = 7–10 Hz; Ø = 4–7 Hz; ∂ = 2–4 Hz) separated by pulse frequency (columns) for ipsilateral (top row) and contralateral (bottom row) ECoG. Note the preferential increase in Ø* and β ECoG power regardless of the pulse frequency. Shaded error represents + SEM (n = 76/77 [3 Hz], 107/195 [8 Hz], 33/38 [12 Hz], and 78/55 [20 Hz] laser/sham events from 5 trials [3 Hz, 12 Hz, and 20 Hz] or 7 trials [8 Hz], 3 STG animals. See also Movie S3.).
See also Figures S1–S3 and Table S1.

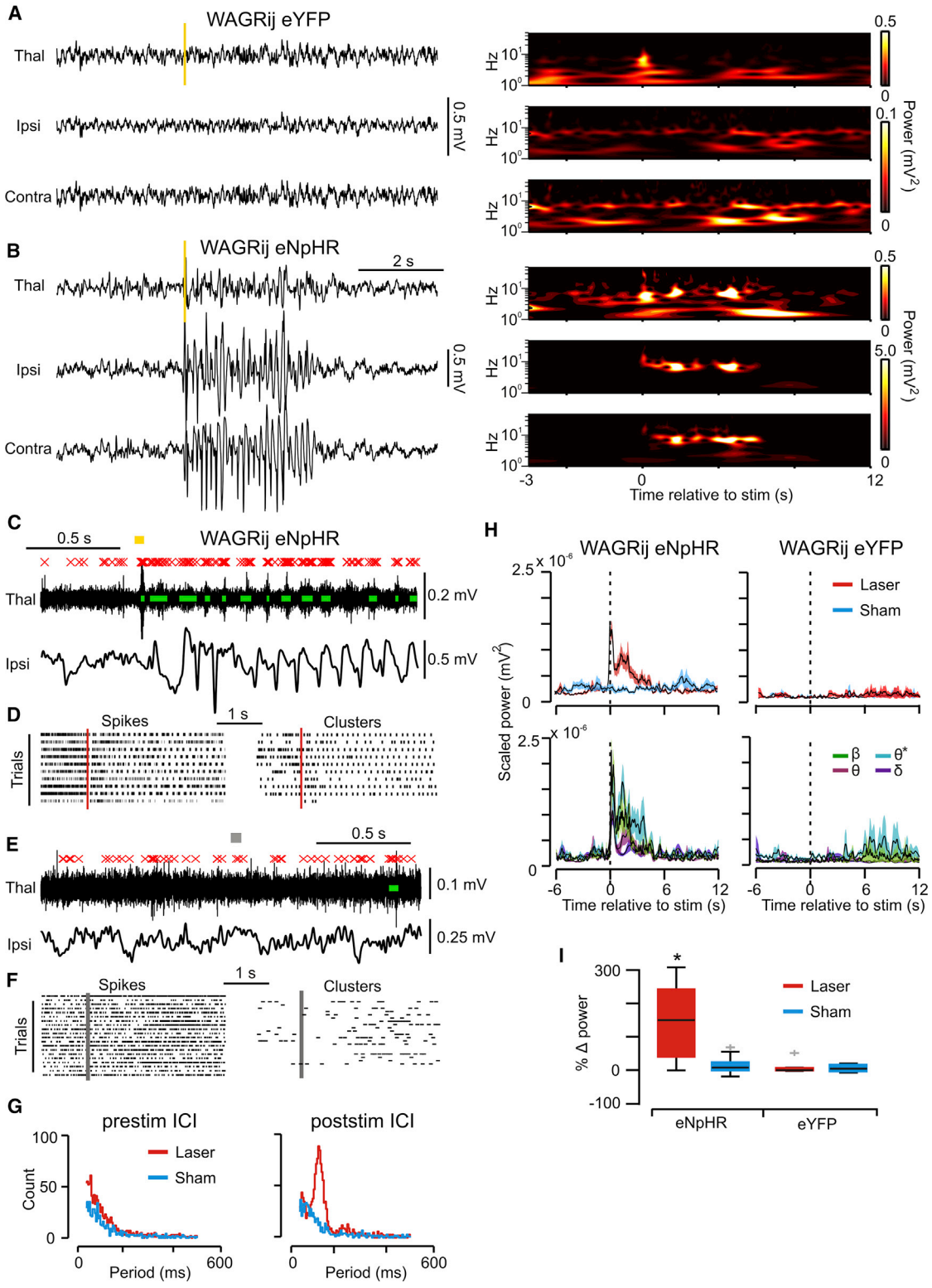

Figure 5. Single 50 ms 594 nm Pulse Induces 8 Hz TC Clusters and Bilateral Seizures

(A) Left: thalamic LFP (top) and cortical ECoG (middle and bottom) from WAGRij-eYFP demonstrating no effect of 50 ms 594 nm pulse (yellow bar) on cortical ECoG. Right: wavelet transformations of traces. Notice the transient increase in power in the thalamic LFP due to the light artifact.

(B) Same as (A), but for WAGRij-eNpHR. The 50 ms light pulse induces a seizure that almost instantly generalizes bilaterally.

(legend continued on next page)

"normal" excitatory inputs to the thalamus cause an abnormally large population of VB cells to fire, which promotes SWDs (Paz et al., 2011).

Origins of the Phasic Firing during SWDs

The in vivo TC clustered spiking following photoinhibition is likely due to a combination of single action potentials and PIR bursts. Although intracellular recordings are required to isolate the relative contribution of single cell bursts to population clusters, the latency between the end of the 594 nm pulse and the start of the spike cluster was similar to the latency of PIR bursts obtained in slices (Figures 1A, 1C, and 3G; Figure S1A). Therefore, the TC clustered spiking that we observe during SWDs could be due in part to T-channel-mediated PIR bursts.

Nonetheless, independent of the origin of the clustered spiking, the major point of this study is that, at the population level, TC activity is heightened and organized into phasic, rhythmic bouts during seizures and that this phasic firing is necessary for seizure maintenance. This last point is supported by our SSFO results, which demonstrate that even unilaterally disrupting phasic firing halts SWDs. While the effects of SSFO may be partially attributed to an increase in TC firing rate, we observed a significant increase in TC firing rate during spontaneous seizures (Figure 2) compared to pre-seizure periods, which corroborates our hypothesis that it is the phasic firing mode of the TC network that is relevant for seizure expression and that seizures depend on more than just reciprocal excitatory feedback between cortex and thalamus. Moreover, our finding that closed-loop eNpHR-mediated reduction of TC output shortens SWDs (Figure S6) further supports our hypothesis.

Our Results in Light of the Controversy

Dissecting the causal involvement of the TC versus CT pathways in rhythmic oscillations has been challenging given their highly reciprocal connections (Jones, 2002; Adams et al., 1997), and traditional, non-specific approaches, such as lesions or electrical stimulation, have yielded conflicting results. Thus, the active role of TC output—in particular, TC cell bursts—in SWDs has been debated (Avanzini et al., 1996; de Curtis and Avanzini, 1994; Tsakiridou et al., 1995; Polack et al., 2007, 2009; Meeren et al., 2002; Danober et al., 1998; Manning et al., 2004; Pinault et al., 1998, 2006).

Many studies have shown that TC neurons are essentially silent or only fire sparse single action potentials throughout SWDs in vivo (Timofeev and Steriade, 2004; Steriade and Contreras, 1995; Polack and Charpier, 2006; Polack et al., 2007; Pinault, 2003; Pinault et al., 1998). These studies, corroborated by findings that pharmacological manipulations of the cortex, but not the thalamus, block SWDs (Polack et al., 2009; Manning et al., 2004; Sitnikova and van Luijtelaar, 2004; Leresche et al., 1998), have resulted in the hypothesis that TC output is not required for SWD initiation or maintenance. Our results refute this theory, as we have shown that TC neurons are highly active and organized into rhythmic, phasic clusters during SWDs and that even unilaterally disrupting TC phasic firing bilaterally alters seizure dynamics. One potential reason our results contrast with those of previous in vivo studies is that stable and high-quality intracellular recordings of TC neurons have required anesthesia or neuroleptanalgesia, which may affect CTC dynamics.

Our Results in Light of the Cortical-Focus Theory

A popular hypothesis that has emerged over the last 10–15 years is that absence seizures are initiated in the cortex—specifically in the somatosensory cortex (S1) in rodents (Meeren et al., 2002, 2005; Polack et al., 2009; Lüttjohann et al., 2013)—known as the "cortical focus theory." Our results do not argue against the cortical focus theory but instead emphasize that TC neurons themselves are able to rapidly recruit epileptic cortical networks. Our results tie the previous controversies regarding which cellular substrates are required for an SWD by suggesting that either CT or TC neurons can be causally involved in SWD initiation by recruiting inhibitory RT neurons that toggle TC phasic firing, a feature that we have shown to be necessary for the maintenance of cortical SWDs and associated absence behavior.

Translational Relevance and Opportunities

We propose that TC phasic firing is a potential therapeutic target to abort or possibly prevent SWDs. Given that T-type calcium channels are mainly responsible for TC burst behavior (Beenhakker and Huguenard, 2009), we propose that designing drugs to specifically target these channels (primarily Cav3.1, the major T-channel in TC neurons) (Talley et al., 1999) would lead to an effective anti-absence therapy and may reduce side effects associated with non-specific anti-absence medication, such as ethosuximide, which also acts on Na^+ channels (Leresche et al., 1998).

Our results are in agreement with complementary findings that systemic or intra-thalamic administration of agents that increase GABAergic inhibition and hyperpolarize neurons (e.g., vigabatrin and tiagabin) promotes burst firing and initiates or worsens SWDs in humans and rodents with epilepsy (Cope et al., 2009; Danober et al., 1998; Hosford and Wang, 1997). Thus, an optimal

(C) In vivo thalamic MU activity during the same event as in (B) (red X's, detected spikes; green bars, detected clusters; yellow bar, 594 nm light). Bottom: ipsilateral ECoG from (B). Note that ECoG spikes phase and time-lock to clusters.
(D) Spike (left) and cluster (right) rasters of all 594 nm events from same animal/trial as in (B) (red bar = 594 nm onset).
(E and F) Same as (C) and (D), but for sham pulses.
(G) Inter-cluster interval (ICI) histograms across all pulses/animals for laser/sham pulses 2 s before (left) or after (right) the pulse onset. Poststim ICI peaks at ~125 ms or 8 Hz.
(H) Top: mean ± SEM, BB power across laser/sham pulses for WAGRij-eNpHR (left) and WAGRij-eYFP (right). Bottom: mean ± SEM, band-specific power across laser pulses. Note that Ø* power remains elevated longer compared to other bands.
(I) Percent change in BB power from prestim to stim periods for all WAGRij-eNpHR and WAGRij-eYFP (red, laser; blue, sham). 594 nm pulses produced a change in BB power, but only in eNpHR rats ($p < 0.05$, ANOVA; eNpHR: 15 trials, 4 animals; eYFP: 13 trials, 4 animals).
See also Figure S3 and Table S1.

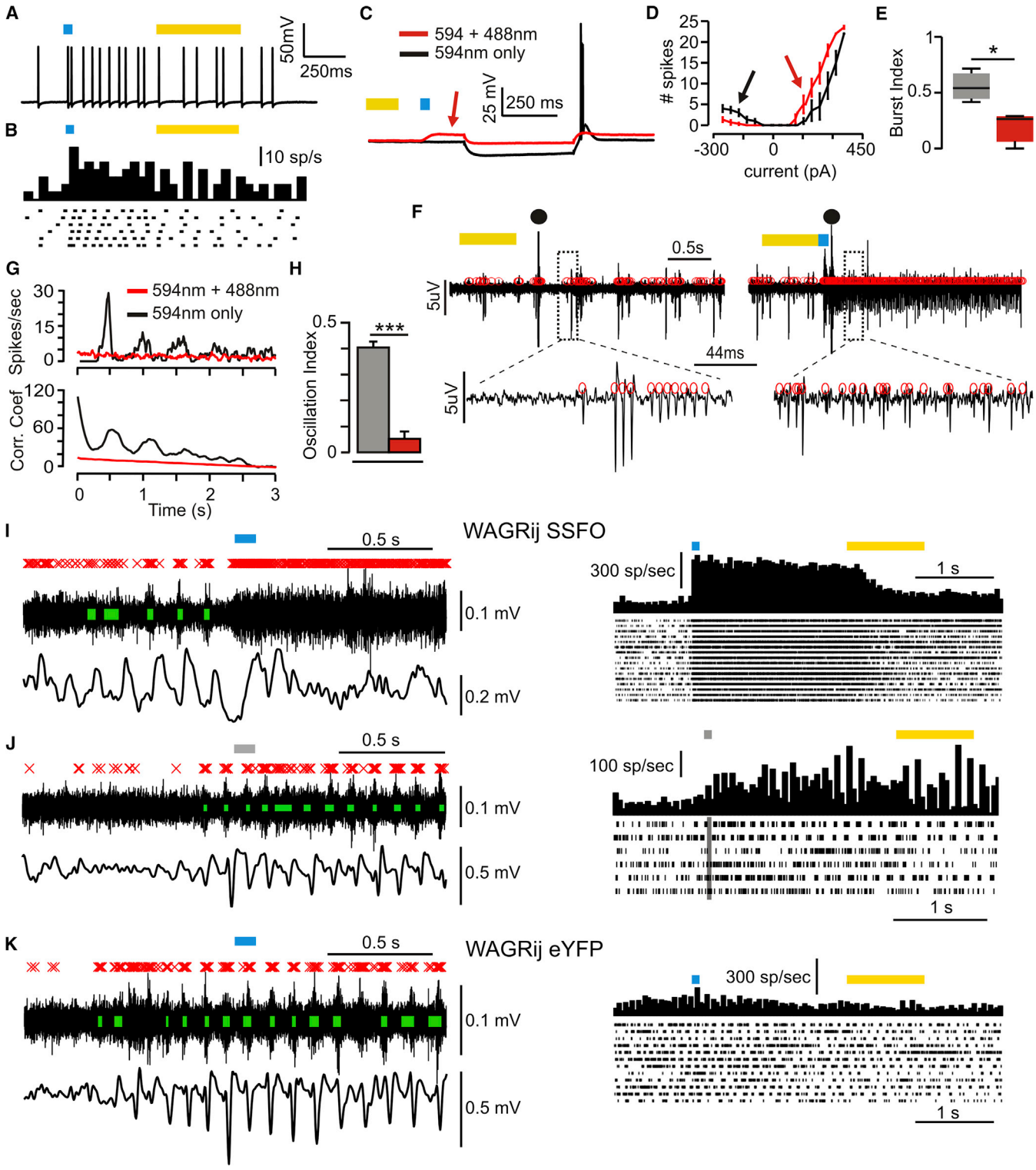

Figure 6. SSFO Activation in TC Neurons Increases Tonic Firing and Reduces Phasic Clusters

(A) Example in vitro whole-cell patch recording from an SSFO-expressing TC neuron demonstrating increased firing rate with SSFO activation (blue bar).

(B) Raster and PSTH of same experiment as (A) over many sweeps.

(C) −150 pA current pulse in SSFO-inactive (594 nm light, black) or SSFO-active (594 nm + 488 nm light, red) sweeps. SSFO activation depolarizes the cell (red arrow) and abolishes the rebound burst.

(legend continued on next page)

therapy would consist of an online switch from a phasic to a tonic TC firing state at the onset of or just prior to the SWD. Until such closed-loop therapies are available, systemic administration of drugs that specifically target phasic TC firing could be used to prevent seizures.

Altering Firing States as a Tool for Controlling Global Networks

We have shown that the firing mode of TC neurons can control global cortical rhythms and that such firing modes can be manipulated in real time for large-scale control of brain state. With tools such as SSFO, we are able to rapidly alter the firing mode of specific neurons, which may not necessarily be replicated by other optogenetic constructs with fast kinetics, such as ChR2. SSFO in particular is an extremely sensitive and powerful tool to investigate the causal sources of other healthy and pathological brain states in real time and to assess the effects of manipulating brain regions that have multi-modal firing states. For instance, one could investigate the role of burst versus tonic output of cerebellar purkinje neurons on motor control or the effects of disrupting hippocampal or cortical bursts during sleep.

Remaining Challenges: Finding Key Cells within Brain-wide Circuits

The ability to selectively target specific cells in complex networks with powerful tools such as optogenetics is crucial for understanding and modifying pathologies, including epilepsy. Although seizures can initiate focally, they rapidly engage widespread circuits; thus, disrupting this spread requires identifying "choke points" that may not necessarily be the seizure foci. Although there might be other targets, we propose that the TC pathway is a choke point for SWDs, similar to the subthalamus for Parkinson's disease (for review, see Paz and Huguenard, 2015).

EXPERIMENTAL PROCEDURES

We performed all experiments according to protocols approved by the Institutional Animal Care and Use Committee; precautions were taken to minimize stress and the number of animals used in each set of experiments. Animals were separately housed after viral injections and surgical implants.

Viral Injections

Stereotactic viral injections were carried out as described (Paz et al., 2011, 2013). 500 nL of concentrated virus (2×10^{12} genome copies per milliliter) carrying genes for eNpHR3.0 (rAAV5/CaMKIIα-eNpHR-EYFP), SSFO (rAAV5/CaMKIIα-SSFO-EYFP), or eYFP alone (rAAV5/CaMKIIα-EYFP) was injected stereotaxically into the right somatosensory thalamus (VB) of postnatal day 30–90 (P30–P90) mice and rats with a 34-gauge beveled needle at 120 nL/min. Injection of viral DNA under CaMKIIα promoter results in expression only in excitatory TC neurons (Gradinaru et al., 2010; Paz et al., 2011, 2013). The stereotaxic coordinates of the injections were 2.6–2.7 mm posterior, 2.8 mm lateral, and 5.8–6.0 mm ventral (rats) or 1.7 mm posterior, 1.5 mm lateral, and 3.5 mm ventral (mice) relative to Bregma (Figure S7).

Slice Preparation

Mice and rats were anesthetized with pentobarbital (100 mg/kg, intraperitoneal) and decapitated. The thalamic slice preparation was performed as described (Paz et al., 2011, 2013). For in vitro recordings from SSFO-expressing animals containing chronic implants, the animals were anesthetized and perfused with ice-cold oxygenated sucrose solution. Implants were then pulled off orthogonal to the skull prior to decapitation. All in vitro SSFO experiments were performed in the dark to avoid chronic activation of SSFO.

Extracellular Thalamic Oscillations

400 μm horizontal slices containing TC and RT were placed in a humidified, oxygenated interface chamber and perfused at a rate of 2 mL/min at 34°C with oxygenated ACSF supplemented with 300 μM glutamine. Oscillations were evoked by a square current pulse (240–260 μA, 30 μs duration) delivered to the internal capsule every 35 s through two parallel tungsten electrodes (50–100 kΩ, FHC) 50–100 μm apart. Extracellular potentials were recorded with a tungsten electrode placed in the VB. Signals were amplified at 10,000× and band-pass filtered between 10 Hz and 10 kHz. Photostimulation of thalamocortical neurons in TC consisted a pulse of 594 nm light (1,000 ms, 2.6 mW), immediately followed by a pulse of 488 nm light (100 ms, 1.2 mW) on every other sweep. Sweeps with current stimulation were immediately followed by sweeps that consisted of photostimulation, but no current stimulation, to determine whether photostimulation alone could sufficiently elicit thalamocortical oscillations. Alternating sweeps were repeated 10–20 times in a single recording.

Patch-Clamp Electrophysiology from Thalamic Slices

Recordings were performed as described (Paz et al., 2011, 2013). Recording electrodes made of borosilicate glass had a resistance of 2.5–4 MΩ when filled with intracellular solution. Potentials were corrected for −15 mV liquid junction potential. Access resistance was monitored in all the recordings, and cells were included for analysis only if the access resistance was <18 MΩ and resistivity change was <20% over the course of the experiment. Cells were filled with 0.2%–0.5% biocytin (Sigma-Aldrich), and whole slices were fixed and processed using standard avidin-biotin peroxidase (Horikawa and Armstrong, 1988). Immunofluorescence was assessed with a laser confocal microscope (Zeiss LSM 510). Numerical values are given as means ± SEM, unless stated otherwise. Data analysis was performed with MATLAB 2013a and Origin 8.0 (Microcal Software).

To quantify changes in burst probability from neurons expressing SSFO by activation with 488 nm light, we injected currents ranging from −250 pA to 350 pA and developed a burst index (see Figure 6E) defined as:

$$BI = 1 - \left[\left| \frac{I_R}{\sqrt{SR_R}} \right| \times \left(\left| \frac{I_R}{\sqrt{SR_R}} \right| + \frac{I_T}{\sqrt{SR_T}} \right)^{-1} \right]$$

(D) Total number of spikes versus injected current for SSFO inactivated (SSFOi) and activated (SSFOa) sweeps. SSFO activation increases the rebound-spike threshold and reduces the number of rebound spikes (black arrow) but inversely affects tonic spiking (red arrow).
(E) Burst index (BI) for SSFOi and SSFOa cells ($p < 0.05$, Wilcoxon rank-sum, $n = 3$ cells).
(F) Extracellular multi-unit activity (red circles, spikes) from thalamic slice showing oscillatory multi-unit clusters following electrical stimulation (●) without SSFO activation (left) and non-oscillatory, desynchronized multi-unit tonic firing with SSFO activation (right).
(G) Top: average PSTHs of extracellular multi-unit activity across SSFO active and inactive sweeps. Bottom: autocorrelations of the PSTHs.
(H) Average oscillatory index (OI) for each condition ($p < 0.001$, t test, $n = 17$ slices).
(I) Left: in vivo thalamic multi-unit activity (top; red X's, spikes; green bars, clusters) and cortical ECoG (bottom) during a closed-loop experiment in WAGRij-SSFO. Clusters and ECoG oscillations at the seizure start are abolished with SSFO activation. Right: PSTH and raster of spikes across all detected seizures with laser activation from same trial.
(J) Same as (I), but for sham pulses.
(K) Same as (I), but for WAGRij-eYFP control.
See also Figures S4 and S5.

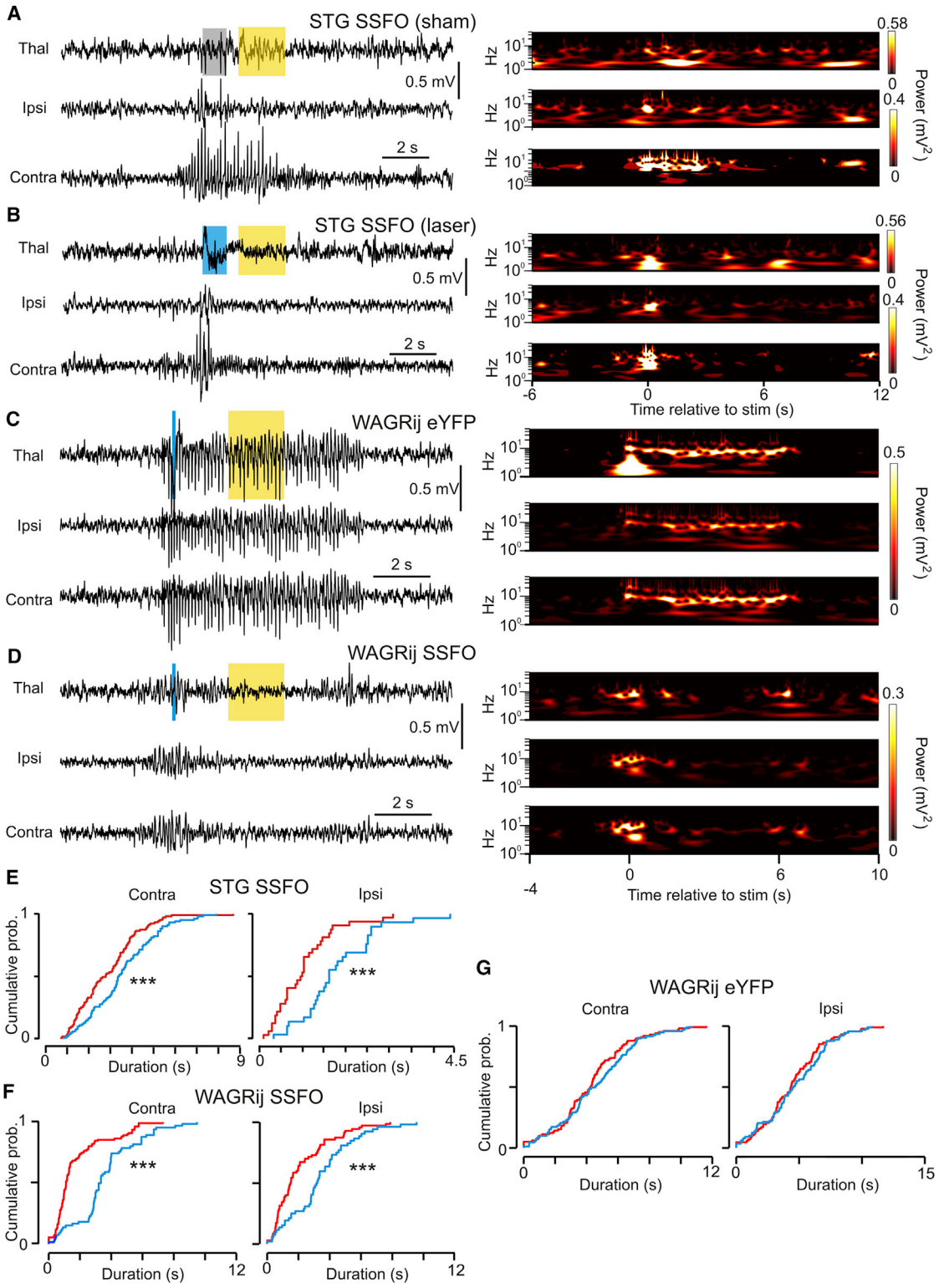

Figure 7. SSFO Activation in TC Cells Aborts Automatically Detected Seizures in STG and WAGRij

(A) Left: example seizure from an SSFO-expressing STG mouse showing thalamic LFP (top), ipsilateral (middle), and contralateral (bottom) ECoG. Gray/yellow bars, sham/594 nm light. Right: wavelet transformations of the channels.

(B) Same as (A), but with a 488 nm pulse that interrupts the seizure. Blue/yellow bars, 488 nm/594 nm light. Right: wavelet transformations; note the silence following the blue pulse.

(legend continued on next page)

where I_R is the negative current threshold for eliciting a rebound burst, I_T is the positive current threshold for eliciting tonic firing, SR_R is burst spike count divided by the current pulse length, and SR_T is the tonic spike count divided by the current pulse length.

In Vivo Data Acquisition

ECoG and LFP signals were recorded using XLTek (Natus Medical Incorporated) or RZ5 (TDT) and sampled at 500 and 2,441 Hz, respectively, while thalamic extracellular multi-unit signals were recorded using Axoscope (Molecular Devices) or RZ5 at 10 and 24 kHz. Two contralateral and two ipsilateral ECoG channels and four thalamic MU/LFP channels were obtained via an implanted optrode (Yizhar et al., 2011; Anikeeva et al., 2011) (see Supplemental Experimental Procedures). A small video camera mounted on a flexible arm was used to continuously monitor the animals. Each recording trial lasted 20–60 min. To control for circadian rhythms, we housed our animals using a regular light/dark cycle and performed recordings from roughly 9:00 a.m. to 4:00 p.m.

Spike Detection and Oscillation Analysis

We first differentiated and smoothed raw MU data, then calculated baseline RMS values to detect spikes via threshold crossing. Spikes were excluded if their waveforms lasted longer than 2 ms (in vitro) or 1 ms (in vivo), and artifact rejection was implemented to eliminate detected signals that were 10-fold larger in amplitude than the mean spike amplitude. We define the various firing modes of the TC network that were detected as follows: (1) burst firing—the intrinsic generation of bursts of action potentials driven by T-type calcium channels (Coulter et al., 1989), (2) clustered spiking—refers to the coordinated and time delimited phasic action potential firing of a population of TC neurons, likely but not necessarily composed of individual TC burst responses, (3) tonic firing—unclustered action potential firing, and (4) phasic firing—the rhythmic occurrence of well-defined MU clusters in a sustained oscillation.

In vitro and in vivo clustered spikes were determined as periods containing at least four spikes within 10 ms with spike rates greater than two times the spike rates of adjacent 40 ms periods of MU activity, as typical rhythmic activity occurs in isolated bouts of firing (see Figures 2A and 6I–6K for examples). In vitro oscillations were determined as periods containing at least two clusters within 600 ms. For each sweep, spikes were aligned to the stimulus onset, a peri-stimulus time histograms (PSTH) with a bin width of 10 ms was calculated, and the PSTH auto-correlation was used to calculate the oscillatory index. OI was defined as:

$$OI = 1 - \left[\frac{t_i}{\left(\frac{p_i + p_{i+1}}{2}\right)}\right]; i \in [2, 4]$$

where t_i = the i^{th} local minimum of the auto-correlation (trough) and p_i = the i^{th} local maximum of the auto-correlation (peak). See Figures 6C and 6D and Figure S5 for details.

For in vivo recordings, we also rejected high-frequency movement artifacts by following previous methods (Paralikar et al., 2009). We then organized spikes into sweeps of 18 s surrounding each seizure and calculated PSTHs using a bin width of 40 ms as well as cluster statistics for laser/sham groups (see Figures 2, 4, 5; Figures S4–S6).

In Vivo Optogenetics

We simultaneously passed a fiber optic with an inline rotating joint (Doric) through a concentric channel in the electrical commutator and connected it to the 200 μm core fiber optic in each animal's headpiece while recording ECoG/MU. The fiber optic was connected to a 488 nm/594 nm dual-wavelength laser control box, which was triggered externally using the RZ5 and custom software. The tip of the fiber rested 200 μm from the most dorsal tungsten electrode on each optrode to allow maximal activation of the TC without physically obstructing the electrodes. We used 8 mW (mice) and 15 mW (rats) of 594 nm/488 nm power, measured at the end of the optical fiber prior to connecting to the animals.

During induced-seizure experiments, our software periodically triggered either 594 nm light or sham pulses (pulses that did not open our laser shutter), selected at random from a uniform distribution, while recording the digital-out from the TDT system. We used different protocols to deliver either a single 50 ms pulse or 25 ms pulses at 3, 8, 12, or 20 Hz, each composed of 50 pulses per train except for the 3 Hz train, which was composed of 20 pulses. A 30 or 60 s time out was implemented after each trigger.

For closed-loop experiments, we wrote custom software to calculate line length (Paz et al., 2013) from an ECoG channel to trigger either a laser or a sham pulse based on threshold crossing. Briefly, line length was calculated by splitting signal into two streams, band-pass filtering between 7–9 Hz or 14–18 Hz, summed, and finally applying a 1 s moving average window. Upon user-defined threshold crossing, a 1 s 594 nm/sham pulse (eNpHR trials) or 100 ms 488 nm/sham pulse and then a 2 s 594 nm pulse (SSFO trials) were delivered, followed by a 15 s time out. We detected seizures in ~585 ms on average.

ECoG Spectral Analysis

We used the continuous wavelet transformation for spectral analysis (Torrence and Compo, 1998) to decompose signals into both time and frequency. We used a basis of Morlet wavelets from 1–128 Hz with seven octaves and ten wavelets per octave. We analyzed individual frequency bands defined by the equation:

$$BV_s = \frac{\partial_j \partial_t}{C_\partial} \sum_{s=l}^{u} \frac{P_s}{S_s}$$

where BV is the band-specific variance (or power), l and u are the lower and upper boundaries of the bandwidth of choice, ∂_j is a scalar for the number of sub-octaves used, ∂_t is our sampling interval, C_∂ is a scalar for the Morlet wavelet, P is total wavelet power, and S is an array containing the scales from the wavelet transform (Torrence and Compo, 1998). Although we did not Z score normalize raw signals, seizure power is relative to the overall power of each recording session. Further, the equation for calculating BV normalizes wavelet power for each scale by the scale itself, and our statistics were based on relative changes in BV on a per-seizure basis, not on absolute BV or wavelet power.

To compare the effects of light on seizure power in both induced and interrupted trials, we calculated relative changes in seizure-averaged BV between pre-stimulus (prestim), stimulus (stim), and post-stimulus (poststim) periods across recording trials (Figures 3D and 3H). We focused on five bandwidths for our analyses: BB (2–20 Hz), β (10–20 Hz), Ø* (7–10 Hz), Ø (4–6 Hz), and ∂ (2–4 Hz), as these bands have been studied extensively in previous epilepsy literature. For induced trials, prestim was defined as 6 s before stim onset; stim periods were defined by the start and end of the pulse train, which were 6.67 s (3 Hz), 6.25 s (8 Hz), 6 s (single pulse), 4.17 s (12 Hz), or 2.5 s (20 Hz) long; and poststim was defined as 6 s after the end of the stim period. We calculated relative changes in BV from prestim to stim for laser and sham and repeated this analysis for each pulse condition to statistically evaluate the effect of various pulse frequencies (Figure 4H).

(C) Detected seizure from WAGRij-eYFP control + 488 nm/594 nm light. Blue light has no effect on the seizure. Note the light artifact in the thalamic wavelet power.
(D) Detected seizure from WAGRij SSFO + 488 nm/594 nm light. Like (B), the wavelet power is abolished following blue light.
(E) Contralateral (left) and ipsilateral (right) empirical cumulative distributions of ECoG total seizure durations across all laser (red) and sham (blue) pulses for STG-SSFO. Laser seizure durations for ipsi- and contralateral cortices were significantly shortened ($p < 0.001$, Kolmogorov-Smirnov test; 110/112 laser/sham seizures, 4 trials, 4 animals).
(F and G) Same as (E), but for WAGRij-SSFO (F, $p < 0.001$, 155/111 laser/sham seizures, 10 trials, 3 animals) and WAGRij-eYFP (G, ns, 96/98 laser/sham seizures, 13 trials, 3 animals. See also Movies S4 and S5.).
See also Figures S4 and S5 and Table S2.

Seizure Length Statistics

Seizure lengths were compared between laser and sham pulses during closed-loop experiments to characterize the effect of SSFO activation. Seizure durations were semi-automatically computed as periods in which BB power crossed and remained above a significance threshold (0.99, calculated from the wavelet transformation) for longer than 1.5 s. Seizures were considered to end if BB power returned to and stayed at baseline levels for longer than 1 s. Post-stimulus seizure lengths were calculated by subtracting the time of the stimulus onset relative to the start of the seizure from the total seizure length.

Seizure lengths were separated between laser and sham seizures and were averaged for each recording session. Summary statistics (Table S2) and cumulative distributions of these statistics (Figure 7) for laser/sham groups were calculated and statistically compared via the Kolmogorov-Smirnov test.

Seizure Probability Statistics

For short 8 Hz (Figures 3E–3H) and single pulse (Figure 5) eNpHR activation experiments, we calculated the probability of inducing a seizure by counting the number of instances in which a seizure (measured via ECoG recordings) occurred within 2 s following a sham or laser trigger and assessed the differences using the Kruskal-Wallis test (see Figure S3).

SUPPLEMENTAL INFORMATION

Supplemental Information includes Supplemental Experimental Procedures, seven figures, two tables, and five movies and can be found with this article online at http://dx.doi.org/10.1016/j.neuron.2016.11.026.

AUTHOR CONTRIBUTIONS

Conceptualization, J.T.P., J.R.H., and J.M.S.; Methodology, J.T.P., J.M.S., and T.J.D.; Software, J.M.S., E.F., T.J.D., and J.R.H.; Formal Analysis, J.M.S. and E.F.; Investigation, J.T.P., J.M.S., and A.M.A.; Validation, J.T.P. and J.M.S.; Resources, K.D. and J.R.H.; Writing – Original Draft, J.M.S., J.T.P., and J.R.H.; Writing – Review & Editing, J.M.S., J.T.P., and J.R.H.; Visualization, J.M.S. and J.T.P.; Supervision, J.T.P. and J.R.H.; Funding Acquisition, J.T.P. and J.R.H.

ACKNOWLEDGMENTS

J.T.P. is supported by NIH-NINDS R00NS078118-01 and Gladstone Institutes. J.R.H. is supported by NIH-NINDS 5R01NS034774. J.T.P. and J.R.H. are supported by a Julie's Hope Challenge Award from CURE, Citizens United for Research in Epilepsy. J.S. is supported by the Stanford Neuroscience Graduate program (grant: 5T32MH020016). K.D. is supported by Howard Hughes Medical Institute, CIRM, NIH, and DARPA REPAIR Program. We thank Carl Pisaturo for designing and fabricating custom electronics, Jessica Wong for her help with animal husbandry, and Stefanie Ritter-Makinson for critical feedback on the manuscript.

Received: July 15, 2016
Revised: September 18, 2016
Accepted: November 7, 2016
Published: December 15, 2016

REFERENCES

Adams, N.C., Lozsádi, D.A., and Guillery, R.W. (1997). Complexities in the thalamocortical and corticothalamic pathways. Eur. J. Neurosci. *9*, 204–209.

Anikeeva, P., Andalman, A.S., Witten, I., Warden, M., Goshen, I., Grosenick, L., Gunaydin, L.A., Frank, L.M., and Deisseroth, K. (2011). Optetrode: a multichannel readout for optogenetic control in freely moving mice. Nat. Neurosci. *15*, 163–170.

Armstrong, C., Krook-Magnuson, E., Oijala, M., and Soltesz, I. (2013). Closed-loop optogenetic intervention in mice. Nat. Protoc. *8*, 1475–1493.

Avanzini, G., Vergnes, M., Spreafico, R., and Marescaux, C. (1993). Calcium-dependent regulation of genetically determined spike and waves by the reticular thalamic nucleus of rats. Epilepsia *34*, 1–7.

Avanzini, G., de Curtis, M., Franceschetti, S., Sancini, G., and Spreafico, R. (1996). Cortical versus thalamic mechanisms underlying spike and wave discharges in GAERS. Epilepsy Res. *26*, 37–44.

Beenhakker, M.P., and Huguenard, J.R. (2009). Neurons that fire together also conspire together: is normal sleep circuitry hijacked to generate epilepsy? Neuron *62*, 612–632.

Berényi, A., Belluscio, M., Mao, D., and Buzsáki, G. (2012). Closed-loop control of epilepsy by transcranial electrical stimulation. Science *337*, 735–737.

Buzsáki, G., and Moser, E.I. (2013). Memory, navigation and theta rhythm in the hippocampal-entorhinal system. Nat. Neurosci. *16*, 130–138.

Buzsáki, G., and Watson, B.O. (2012). Brain rhythms and neural syntax: implications for efficient coding of cognitive content and neuropsychiatric disease. Dialogues Clin. Neurosci. *14*, 345–367.

Buzsáki, G., Bickford, R.G., Ponomareff, G., Thal, L.J., Mandel, R., and Gage, F.H. (1988). Nucleus basalis and thalamic control of neocortical activity in the freely moving rat. J. Neurosci. *8*, 4007–4026.

Castro-Alamancos, M.A. (2004). Dynamics of sensory thalamocortical synaptic networks during information processing states. Prog. Neurobiol. *74*, 213–247.

Chmielowska, J., Carvell, G.E., and Simons, D.J. (1989). Spatial organization of thalamocortical and corticothalamic projection systems in the rat SmI barrel cortex. J. Comp. Neurol. *285*, 325–338.

Coenen, A.M., Drinkenburg, W.H., Inoue, M., and van Luijtelaar, E.L. (1992). Genetic models of absence epilepsy, with emphasis on the WAG/Rij strain of rats. Epilepsy Res. *12*, 75–86.

Contreras, D., and Steriade, M. (1995). Cellular basis of EEG slow rhythms: a study of dynamic corticothalamic relationships. J. Neurosci. *15*, 604–622.

Cope, D.W., Di Giovanni, G., Fyson, S.J., Orbán, G., Errington, A.C., Lorincz, M.L., Gould, T.M., Carter, D.A., and Crunelli, V. (2009). Enhanced tonic GABAA inhibition in typical absence epilepsy. Nat. Med. *15*, 1392–1398.

Coulter, D.A., Huguenard, J.R., and Prince, D.A. (1989). Calcium currents in rat thalamocortical relay neurones: kinetic properties of the transient, low-threshold current. J. Physiol. *414*, 587–604.

Cox, C.L., Huguenard, J.R., and Prince, D.A. (1997). Nucleus reticularis neurons mediate diverse inhibitory effects in thalamus. Proc. Natl. Acad. Sci. USA *94*, 8854–8859.

Danober, L., Depaulis, A., Marescaux, C., and Vergnes, M. (1993). Effects of cholinergic drugs on genetic absence seizures in rats. Eur. J. Pharmacol. *234*, 263–268.

Danober, L., Deransart, C., Depaulis, A., Vergnes, M., and Marescaux, C. (1998). Pathophysiological mechanisms of genetic absence epilepsy in the rat. Prog. Neurobiol. *55*, 27–57.

de Curtis, M., and Avanzini, G. (1994). Thalamic regulation of epileptic spike and wave discharges. Funct. Neurol. *9*, 307–326.

Dreyfus, F.M., Tscherter, A., Errington, A.C., Renger, J.J., Shin, H.S., Uebele, V.N., Crunelli, V., Lambert, R.C., and Leresche, N. (2010). Selective T-type calcium channel block in thalamic neurons reveals channel redundancy and physiological impact of I(T)window. J. Neurosci. *30*, 99–109.

Gomora, J.C., Daud, A.N., Weiergräber, M., and Perez-Reyes, E. (2001). Block of cloned human T-type calcium channels by succinimide antiepileptic drugs. Mol. Pharmacol. *60*, 1121–1132.

Gradinaru, V., Thompson, K.R., and Deisseroth, K. (2008). eNpHR: a Natronomonas halorhodopsin enhanced for optogenetic applications. Brain Cell Biol. *36*, 129–139.

Gradinaru, V., Zhang, F., Ramakrishnan, C., Mattis, J., Prakash, R., Diester, I., Goshen, I., Thompson, K.R., and Deisseroth, K. (2010). Molecular and cellular approaches for diversifying and extending optogenetics. Cell *141*, 154–165.

Hasselmo, M.E., Bodelón, C., and Wyble, B.P. (2002). A proposed function for hippocampal theta rhythm: separate phases of encoding and retrieval enhance reversal of prior learning. Neural Comput. *14*, 793–817.

Hirata, A., and Castro-Alamancos, M.A. (2010). Neocortex network activation and deactivation states controlled by the thalamus. J. Neurophysiol. *103*, 1147–1157.

Horikawa, K., and Armstrong, W.E. (1988). A versatile means of intracellular labeling: injection of biocytin and its detection with avidin conjugates. J. Neurosci. Methods *25*, 1–11.

Hosford, D.A., and Wang, Y. (1997). Utility of the lethargic (lh/lh) mouse model of absence seizures in predicting the effects of lamotrigine, vigabatrin, tiagabine, gabapentin, and topiramate against human absence seizures. Epilepsia *38*, 408–414.

Huguenard, J.R. (1999). Neuronal circuitry of thalamocortical epilepsy and mechanisms of antiabsence drug action. Adv. Neurol. *79*, 991–999.

Huguenard, J.R. (2002). Block of T-Type Ca(2+) channels is an important action of Succinimide Antiabsence Drugs. Epilepsy Curr. *2*, 49–52.

Huguenard, J.R., and McCormick, D.A. (1992). Simulation of the currents involved in rhythmic oscillations in thalamic relay neurons. J. Neurophysiol. *68*, 1373–1383.

Huguenard, J.R., and McCormick, D.A. (2007). Thalamic synchrony and dynamic regulation of global forebrain oscillations. Trends Neurosci. *30*, 350–356.

Huguenard, J.R., and Prince, D.A. (1994). Intrathalamic rhythmicity studied in vitro: nominal T-current modulation causes robust antioscillatory effects. J. Neurosci. *14*, 5485–5502.

Jahnsen, H., and Llinás, R. (1984). Electrophysiological properties of guinea-pig thalamic neurones: an in vitro study. J. Physiol. *349*, 205–226.

Jones, E.G. (2002). Thalamic circuitry and thalamocortical synchrony. Philos. Trans. R. Soc. Lond. B Biol. Sci. *357*, 1659–1673.

Jones, E.G. (2007). The Thalamus. History (Lond.) *326*, 419–442.

Kostopoulos, G.K. (2000). Spike-and-wave discharges of absence seizures as a transformation of sleep spindles: the continuing development of a hypothesis. Clin. Neurophysiol. *111* (*Suppl 2*), S27–S38.

Kros, L., Rooda, O.H., De Zeeuw, C.I., and Hoebeek, F.E. (2015). Controlling cerebellar output to treat refractory epilepsy. Trends Neurosci. *38*, 787–799.

Lacey, C.J., Bryant, A., Brill, J., and Huguenard, J.R. (2012). Enhanced NMDA receptor-dependent thalamic excitation and network oscillations in stargazer mice. J. Neurosci. *32*, 11067–11081.

Leresche, N., Parri, H.R., Erdemli, G., Guyon, A., Turner, J.P., Williams, S.R., Asprodini, E., and Crunelli, V. (1998). On the action of the anti-absence drug ethosuximide in the rat and cat thalamus. J. Neurosci. *18*, 4842–4853.

Lüttjohann, A., Schoffelen, J.M., and van Luijtelaar, G. (2013). Peri-ictal network dynamics of spike-wave discharges: phase and spectral characteristics. Exp. Neurol. *239*, 235–247.

Manning, J.P.A., Richards, D.A., Leresche, N., Crunelli, V., and Bowery, N.G. (2004). Cortical-area-specific block of genetically determined absence seizures by ethosuximide. Neuroscience *123*, 5–9.

Marescaux, C., Vergnes, M., and Depaulis, A. (1992). Genetic absence epilepsy in rats from Strasbourg–a review. J. Neural Transm. Suppl. *35* (*Suppl.*), 37–69.

McCormick, D.A. (1992). Neurotransmitter actions in the thalamus and cerebral cortex and their role in neuromodulation of thalamocortical activity. Prog. Neurobiol. *39*, 337–388.

McCormick, D.A., McGinley, M.J., and Salkoff, D.B. (2015). Brain state dependent activity in the cortex and thalamus. Curr. Opin. Neurobiol. *31*, 133–140.

Meeren, H.K., Pijn, J.P., Van Luijtelaar, E.L., Coenen, A.M., and Lopes da Silva, F.H. (2002). Cortical focus drives widespread corticothalamic networks during spontaneous absence seizures in rats. J. Neurosci. *22*, 1480–1495.

Meeren, H., van Luijtelaar, G., Lopes da Silva, F., and Coenen, A. (2005). Evolving concepts on the pathophysiology of absence seizures: the cortical focus theory. Arch. Neurol. *62*, 371–376.

Noebels, J.L., Qiao, X., Bronson, R.T., Spencer, C., and Davisson, M.T. (1990). Stargazer: a new neurological mutant on chromosome 15 in the mouse with prolonged cortical seizures. Epilepsy Res. *7*, 129–135.

Paralikar, K.J., Rao, C.R., and Clement, R.S. (2009). New approaches to eliminating common-noise artifacts in recordings from intracortical microelectrode arrays: inter-electrode correlation and virtual referencing. J. Neurosci. Methods *181*, 27–35.

Paz, J.T., and Huguenard, J.R. (2015). Microcircuits and their interactions in epilepsy: is the focus out of focus? Nat. Neurosci. *18*, 351–359.

Paz, J.T., Chavez, M., Saillet, S., Deniau, J.M., and Charpier, S. (2007). Activity of ventral medial thalamic neurons during absence seizures and modulation of cortical paroxysms by the nigrothalamic pathway. J. Neurosci. *27*, 929–941.

Paz, J.T., Bryant, A.S., Peng, K., Fenno, L., Yizhar, O., Frankel, W.N., Deisseroth, K., and Huguenard, J.R. (2011). A new mode of corticothalamic transmission revealed in the Gria4(-/-) model of absence epilepsy. Nat. Neurosci. *14*, 1167–1173.

Paz, J.T., Davidson, T.J., Frechette, E.S., Delord, B., Parada, I., Peng, K., Deisseroth, K., and Huguenard, J.R. (2013). Closed-loop optogenetic control of thalamus as a tool for interrupting seizures after cortical injury. Nat. Neurosci. *16*, 64–70.

Pinault, D. (2003). Cellular interactions in the rat somatosensory thalamocortical system during normal and epileptic 5-9 Hz oscillations. J. Physiol. *552*, 881–905.

Pinault, D., Leresche, N., Charpier, S., Deniau, J.M., Marescaux, C., Vergnes, M., and Crunelli, V. (1998). Intracellular recordings in thalamic neurones during spontaneous spike and wave discharges in rats with absence epilepsy. J. Physiol. *509*, 449–456.

Pinault, D., Slézia, A., and Acsády, L. (2006). Corticothalamic 5-9 Hz oscillations are more pro-epileptogenic than sleep spindles in rats. J. Physiol. *574*, 209–227.

Polack, P.-O., and Charpier, S. (2006). Intracellular activity of cortical and thalamic neurones during high-voltage rhythmic spike discharge in Long-Evans rats in vivo. J. Physiol. *571*, 461–476.

Polack, P.-O., Guillemain, I., Hu, E., Deransart, C., Depaulis, A., and Charpier, S. (2007). Deep layer somatosensory cortical neurons initiate spike-and-wave discharges in a genetic model of absence seizures. J. Neurosci. *27*, 6590–6599.

Polack, P.O., Mahon, S., Chavez, M., and Charpier, S. (2009). Inactivation of the somatosensory cortex prevents paroxysmal oscillations in cortical and related thalamic neurons in a genetic model of absence epilepsy. Cereb. Cortex *19*, 2078–2091.

Poulet, J.F.A., Fernandez, L.M., Crochet, S., and Petersen, C.C. (2012). Thalamic control of cortical states. Nat. Neurosci. *15*, 370–372.

Richards, D.A., Manning, J.P., Barnes, D., Rombola, L., Bowery, N.G., Caccia, S., Leresche, N., and Crunelli, V. (2003). Targeting thalamic nuclei is not sufficient for the full anti-absence action of ethosuximide in a rat model of absence epilepsy. Epilepsy Res. *54*, 97–107.

Sarkisova, K., and van Luijtelaar, G. (2011). The WAG/Rij strain: a genetic animal model of absence epilepsy with comorbidity of depression [corrected]. Prog. Neuropsychopharmacol. Biol. Psychiatry *35*, 854–876.

Sitnikova, E., and van Luijtelaar, G. (2004). Cortical control of generalized absence seizures: effect of lidocaine applied to the somatosensory cortex in WAG/Rij rats. Brain Res. *1012*, 127–137.

Sohal, V.S., Huntsman, M.M., and Huguenard, J.R. (2000). Reciprocal inhibitory connections regulate the spatiotemporal properties of intrathalamic oscillations. J. Neurosci. *20*, 1735–1745.

Steriade, M. (2000). Corticothalamic resonance, states of vigilance and mentation. Neuroscience *101*, 243–276.

Steriade, M., and Contreras, D. (1995). Relations between cortical and thalamic cellular events during transition from sleep patterns to paroxysmal activity. J. Neurosci. *15*, 623–642.

Steriade, M., McCormick, D.A., and Sejnowski, T.J. (1993). Thalamocortical oscillations in the sleeping and aroused brain. Science *262*, 679–685.

Talley, E.M., Cribbs, L.L., Lee, J.H., Daud, A., Perez-Reyes, E., and Bayliss, D.A. (1999). Differential distribution of three members of a gene family encoding low voltage-activated (T-type) calcium channels. J. Neurosci. *19*, 1895–1911.

Timofeev, I., and Steriade, M. (2004). Neocortical seizures: initiation, development and cessation. Neuroscience *123*, 299–336.

Timofeev, I., Grenier, F., and Steriade, M. (1998). Spike-wave complexes and fast components of cortically generated seizures. IV. Paroxysmal fast runs in cortical and thalamic neurons. J. Neurophysiol. *80*, 1495–1513.

Torrence, C., and Compo, G.P. (1998). A practical guide to wavelet analysis. Bull. Am. Meteorol. Soc. *79*, 61–78.

Tsakiridou, E., Bertollini, L., de Curtis, M., Avanzini, G., and Pape, H.C. (1995). Selective increase in T-type calcium conductance of reticular thalamic neurons in a rat model of absence epilepsy. J. Neurosci. *15*, 3110–3117.

van Luijtelaar, E.L.J.M., and Coenen, A.M.L. (1986). Two types of electrocortical paroxysms in an inbred strain of rats. Neurosci. Lett. *70*, 393–397.

van Luijtelaar, G., and Sitnikova, E. (2006). Global and focal aspects of absence epilepsy: the contribution of genetic models. Neurosci. Biobehav. Rev. *30*, 983–1003.

Vergnes, M., and Marescaux, C. (1992). Cortical and thalamic lesions in rats with genetic absence epilepsy. J. Neural Transm. Suppl. *35*, 71–83.

Yizhar, O., Fenno, L.E., Prigge, M., Schneider, F., Davidson, T.J., O'Shea, D.J., Sohal, V.S., Goshen, I., Finkelstein, J., Paz, J.T., et al. (2011). Neocortical excitation/inhibition balance in information processing and social dysfunction. Nature *477*, 171–178.

Zhang, F., Wang, L.P., Boyden, E.S., and Deisseroth, K. (2006). Channelrhodopsin-2 and optical control of excitable cells. Nat. Methods *3*, 785–792.